J. Fluid Mech. (1991), *vol.* 231, *pp.* 211–228
Printed in Great Britain

Boundary effects on electrophoresis of colloidal cylinders

By HUAN J. KEH, KUO D. HORNG AND JIMMY KUO
Department of Chemical Engineering, National Taiwan University, Taipei 10764, Taiwan, Republic of China

(Received 6 December 1990)

An exact analytical study is presented for the electrophoresis of an infinite insulating cylinder in the proximity of an infinite plane wall parallel to its axis. The electric field is exerted perpendicular to the particle axis in two fundamental cases: normal to a conducting plane and parallel to a non-conducting wall. The electrical double layers adjacent to solid surfaces are assumed to be thin with respect to the particle radius and the gap thickness between surfaces. The two-dimensional electrostatic and hydrodynamic governing equations are solved in the quasi-steady limit using bipolar coordinates and the typical electric-field-line, equipotential-line and streamline patterns are exhibited. Corrections to Smoluchowski's equation for the electrophoretic velocities of the particle are determined in simple closed forms as a function of λ, the ratio of particle radius to distance of the particle axis from the wall. Interestingly, the electrophoretic mobility of the cylinder in the direction parallel to a dielectric plane increases monotonically as the particle approaches the wall and becomes infinity when the particle touches the wall. For the motion of a cylinder normal to a conducting plane, the presence of the wall causes a reduction in the electrophoretic velocity, which goes to zero as $\lambda \to 1$. It is found that boundary effects on the electrophoresis of a cylinder are much stronger than for a sphere at the same value of λ. The boundary effects on the particle mobility and on the fluid flow pattern in electrophoresis differ significantly from those of the corresponding sedimentation problem with which comparisons are made.

1. Introduction

When a charged particle suspended in an electrolyte solution is subjected to an external electric field, the particle begins to move. This motion is called electrophoresis and is used in many technical applications. It is well known that a non-conducting particle of arbitrary shape will migrate in an unbounded fluid with a velocity $\boldsymbol{U}_0$ given by the Smoluchowski equation,

$$\boldsymbol{U}_0 = \frac{\epsilon\zeta}{4\pi\eta}\boldsymbol{E}_\infty, \tag{1.1}$$

provided that the local radii of curvature of the particle are much larger than the thickness of the electrical double layer surrounding the particle (Morrison 1970). In this equation, η is the fluid viscosity, ϵ is the fluid permittivity, ζ is the zeta potential of the particle surface and $\boldsymbol{E}_\infty$ is the imposed electric field. There is no rotational motion of the particle. The ratio $\boldsymbol{U}_0/\boldsymbol{E}_\infty$ is known as the electrophetic mobility of the particle.

In addition to the particle movement, the interaction between the electric field and

the ions within the mobile portion of the double layer causes a tangential velocity for the fluid within the diffuse layer. This 'slip velocity' at each point on the surface (or more precisely, on the outer edge of the diffuse layer), relative to the frame of the particle, is given by the Helmholtz expression for the electro-osmotic flow:

$$\boldsymbol{v}_s = -\frac{\epsilon\zeta}{4\pi\eta}\boldsymbol{E}_s. \tag{1.2}$$

Here, $\boldsymbol{E}_s$ is the local electric field which has no normal component for a non-conducting surface with a thin double layer.

In practical applications of electrophoresis to particle analysis or separation, colloidal particles are not isolated and will move in the presence of neighbouring particles and/or boundaries. Recently, much progress has been made in the theoretical analysis concerning the application of (1.1) to charged spheres surrounded by a thin double layer in the proximity of rigid boundaries (Morrison & Stukel 1970; Keh & Anderson 1985; Keh & Chen 1988; Keh & Lien 1991) and other spheres (Reed & Morrison 1976; Chen & Keh 1988; Keh & Yang 1990). An important result of these studies is that the influence of particle interactions and boundary effects on electrophoresis is much weaker than on sedimentation, because the disturbance to the fluid velocity field caused by an electrophoretic sphere decays faster (as r^{-3}) than that caused by a stokeslet (as r^{-1}), where r is the distance from the sphere centre. Another interesting finding of the boundary effects is that the electrophoretic velocity of a sphere near a rigid wall can be even larger than that for an identical sphere undergoing electrophoresis in an unbounded fluid (Keh & Chen 1988; Keh & Lien 1991).

Although the electrophoretic motion of an isolated particle in an unbounded fluid has been investigated for geometries like a circular cylinder (Henry 1931; Morrison 1971; Stigter 1978) or ellipsoid (Teubner 1982; Fair & Anderson 1989; Yoon & Kim 1989), the boundary effect on the electrophoresis of non-spherical particles has not yet been reported. The purpose of this paper is to determine the electrophoretic mobility of an infinite insulating cylinder near a large plane wall parallel to its axis in a transversely applied electric field and compare the results with those for the corresponding electrophoresis of a sphere. The Debye screening length is assumed to be much smaller than the particle radius and the surface-to-surface spacing between the particle and the wall. Thus, the effect considered in the analysis is not due to any interaction between the double layers surrounding the particle and adjacent to the wall.

This paper is presented in five sections. In §2 the general problem of two-dimensional creeping motion of an infinite circular cylinder near an infinite solid plane is exactly solved. Based on this analysis, the electrophoretic motion of a non-conducting cylinder in the direction normal to its axis and parallel to a dielectric plane is examined in §3. The closed-form analytical solution for the translational and angular velocities of the electrophoretic particle in a constant electric field is obtained in (3.17). Section 4 provides the exact solution of a complementary problem to that treated in §3, the electrophoresis of a cylinder in the direction perpendicular to its axis and to a conducting plane. The final result of the wall-corrected electrophoretic mobility for this case is presented in (4.10). In §5, a short summary of this work is given.

2. Creeping motion of a circular cylinder near a planar wall

In this section we consider the two-dimensional creeping motion of an infinite cylinder of radius a in an incompressible viscous fluid near an infinite planar wall located at a distance d from the axis of the cylinder. The cylinder has a translational velocity $U_x\boldsymbol{e}_x+U_y\boldsymbol{e}_y$ and is rotating with an angular velocity $\Omega\boldsymbol{e}_z$, where $\boldsymbol{e}_x$, $\boldsymbol{e}_y$ and $\boldsymbol{e}_z$ are the unit vectors in rectangular coordinates. The planar wall is stationary.

In addition to the Cartesian system (x, y, z), it is also convenient to introduce cylindrical bipolar coordinates (ξ, ψ, z), as illustrated in figure 1. The relationship between these two coordinate systems is (Jeffery 1922; Happel & Brenner 1983)

$$x = \frac{c\sinh\psi}{\cosh\psi-\cos\xi}, \quad y = \frac{c\sin\xi}{\cosh\psi-\cos\xi}, \tag{2.1a, b}$$

where $-\infty < \psi < \infty$, $0 \leqslant \xi < 2\pi$, and c is a characteristic length in the bipolar coordinates which is positive.

The curves ψ = constant correspond to a family of non-intersecting, coaxial circles (or cylinders) whose centres all lie along the x-axis. The special case $\psi = 0$ generates a circle of infinite radius and corresponds to the entire y-axis (or the plane). $\psi = \psi_0 > 0$ represents the circle (or the cylinder) of radius $a = c\,\mathrm{cosech}\,\psi_0$, with its centre at the point $(x = d = c\coth\psi_0, y = 0)$. The ratio of the radius of the cylinder to the distance of the axis of the cylinder from the plane is related to ψ_0 by

$$\lambda = a/d = \mathrm{sech}\,\psi_0. \tag{2.2}$$

The creeping motion and continuity equations are

$$\eta\nabla^2\boldsymbol{v}-\nabla p = \boldsymbol{0} \tag{2.3}$$

and

$$\nabla\cdot\boldsymbol{v} = 0, \tag{2.4}$$

where $\boldsymbol{v}(\boldsymbol{x})$ is the fluid velocity distribution and $p(\boldsymbol{x})$ is the dynamic pressure. Taking the curl of both sides of (2.3) and introducing (2.4) and the stream function result in a fourth-order linear partial differential equation for the stream function Ψ:

$$\nabla^4\Psi = \nabla^2(\nabla^2\Psi) = 0. \tag{2.5}$$

In (2.3)–(2.5),

$$\nabla = \boldsymbol{e}_x\frac{\partial}{\partial x}+\boldsymbol{e}_y\frac{\partial}{\partial y} = \frac{1}{c}(\cosh\psi-\cos\xi)\left(\boldsymbol{e}_\xi\frac{\partial}{\partial\xi}+\boldsymbol{e}_\psi\frac{\partial}{\partial\psi}\right), \tag{2.6a}$$

$$\nabla^2 = \frac{\partial^2}{\partial x^2}+\frac{\partial^2}{\partial y^2} = \frac{1}{c^2}(\cosh\psi-\cos\xi)^2\left(\frac{\partial^2}{\partial\xi^2}+\frac{\partial^2}{\partial\psi^2}\right), \tag{2.6b}$$

where $\boldsymbol{e}_\xi$ and $\boldsymbol{e}_\psi$ are unit vectors in bipolar coordinates. Note that

$$\boldsymbol{e}_x = \frac{1}{\cosh\psi-\cos\xi}\left[-\sinh\psi\sin\xi\,\boldsymbol{e}_\xi-(\cosh\psi\cos\xi-1)\,\boldsymbol{e}_\psi\right], \tag{2.7a}$$

$$\boldsymbol{e}_y = \frac{1}{\cosh\psi-\cos\xi}\left[(\cosh\psi\cos\xi-1)\,\boldsymbol{e}_\xi-\sinh\psi\sin\xi\,\boldsymbol{e}_\psi\right]. \tag{2.7b}$$

The stream function is related to the velocity field in bipolar coordinates by the formulae

$$v_\xi = \frac{1}{c}(\cosh\psi-\cos\xi)\frac{\partial\Psi}{\partial\psi}, \quad v_\psi = -\frac{1}{c}(\cosh\psi-\cos\xi)\frac{\partial\Psi}{\partial\xi}. \tag{2.8a, b}$$

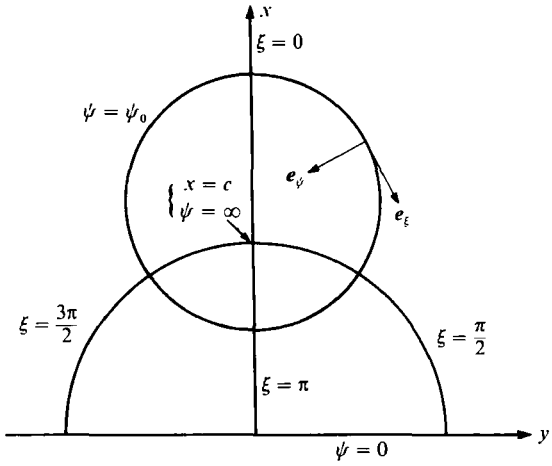

FIGURE 1. Geometrical sketch for the two-dimensional motion of a cylinder in the proximity of a plane wall.

The boundary conditions appropriate to the present problem require that:

$$\boldsymbol{v} = U_x \boldsymbol{e}_x + U_y \boldsymbol{e}_y + \Omega \boldsymbol{e}_z \times a(-\boldsymbol{e}_\psi) \quad \text{at} \quad \psi = \psi_0, \tag{2.9a}$$

$$\boldsymbol{v} = \boldsymbol{0} \quad \text{at} \quad \psi = 0 \text{ (or } x = 0), \tag{2.9b}$$

$$\boldsymbol{v} \to \boldsymbol{0} \quad \text{as} \quad (x^2+y^2)^{\frac{1}{2}} \to \infty \text{ and } x \geqslant 0. \tag{2.9c}$$

In (2.9a), $\boldsymbol{e}_z \times (-\boldsymbol{e}_\psi) = \boldsymbol{e}_\xi$.

A solution of the biharmonic equation (2.5) in bipolar coordinates, suitable for satisfying boundary conditions on the cylinder and plane, has been given by Jeffery (1922) and Wakiya (1975):

$$\begin{aligned}\psi = c(\cosh\psi - \cos\xi)^{-1}\Big[& A\psi(\cosh\psi - \cos\xi) + (B + C\psi)\sinh\psi - D\psi\sin\xi \\ & + \sum_{n=1}^{\infty} \{[a_n \cosh(n+1)\psi + b_n \sinh(n+1)\psi + c_n \cosh(n-1)\psi \\ & + d_n \sinh(n-1)\psi]\cos n\xi \\ & + [a'_n \cosh(n+1)\psi + b'_n \sinh(n+1)\psi + c'_n \cosh(n-1)\psi \\ & + d'_n \sinh(n-1)\psi]\sin n\xi\}\Big].\end{aligned} \tag{2.10}$$

The coefficients A, B, C, D, a_n, b_n, c_n, d_n, a'_n, b'_n, c'_n and d'_n (d_1 and d'_1 are trivial) are found from the boundary conditions given in (2.9) using (2.7) and (2.8). The procedure is straightforward, with the results

$$A = \left(\frac{U_y}{\psi_0} + \frac{a\Omega}{\sinh\psi_0}\right)\coth\psi_0, \quad B = -A, \tag{2.11a, b}$$

$$C = -\frac{U_y}{\psi_0}, \quad D = -\frac{U_x}{\psi_0 - \tanh\psi_0}, \tag{2.11c, d}$$

$$a_1 = -\tfrac{1}{2}A\tanh\psi_0, \quad b_1 = \tfrac{1}{2}A, \quad c_1 = -a_1, \tag{2.11e–g}$$

$$a'_1 = -\tfrac{1}{2}D\tanh\psi_0, \quad b'_1 = \tfrac{1}{2}D, \quad c'_1 = -a'_1, \tag{2.11h–j}$$

$$a_n = b_n = c_n = d_n = a'_n = b'_n = c'_n = d'_n = 0 \quad \text{for} \quad n \geqslant 2. \tag{2.11k}$$

The drag force and torque per unit length exerted by the fluid on the cylinder can be determined from

$$\boldsymbol{F} = -\int_0^{2\pi} [\boldsymbol{e}_\psi \cdot \boldsymbol{\Pi}]_{\psi=\psi_0} \frac{a \sinh \psi_0 \, \mathrm{d}\xi}{\cosh \psi_0 - \cos \xi}, \tag{2.12a}$$

and

$$\boldsymbol{T} = \int_0^{2\pi} [\boldsymbol{e}_\psi \times (\boldsymbol{e}_\psi \cdot \boldsymbol{\Pi})]_{\psi=\psi_0} \frac{a^2 \sinh \psi_0 \, \mathrm{d}\xi}{\cosh \psi_0 - \cos \xi}, \tag{2.12b}$$

respectively. In (2.12), $\boldsymbol{\Pi}$ is the total stress tensor,

$$\boldsymbol{\Pi} = -p\boldsymbol{I} + \eta[\nabla \boldsymbol{v} + (\nabla \boldsymbol{v})^{\mathrm{T}}], \tag{2.13}$$

where $\boldsymbol{I}$ is the unit tensor. Applying (2.10) to the integrals in (2.12) and using (2.6a), (2.8) and (2.13) result in the simple relationships

$$\boldsymbol{F} = 4\pi\eta(D\boldsymbol{e}_x + C\boldsymbol{e}_y), \tag{2.14a}$$

$$\boldsymbol{T} = -4\pi\eta a(A \sinh \psi_0 + C \cosh \psi_0)\, \boldsymbol{e}_z. \tag{2.14b}$$

Substituting (2.11a–d) into (2.14), one has

$$\boldsymbol{F} = -4\pi\eta\left(\frac{U_x}{\psi_0 - \tanh \psi_0}\boldsymbol{e}_x + \frac{U_y}{\psi_0}\boldsymbol{e}_y\right), \tag{2.15a}$$

$$\boldsymbol{T} = -4\pi\eta a^2 \Omega \coth \psi_0 \, \boldsymbol{e}_z. \tag{2.15b}$$

Obviously, as the cylinder approaches the planar wall (with decreasing ψ_0 or increasing λ) its translational and rotational mobilities decrease steadily and vanish at the limit of $\lambda = 1$. Note that, as shown in (2.15), the translation and rotation for this two-dimensional creeping motion are not coupled with each other. Thus, a sedimenting cylinder near a planar wall does not rotate if no external couple is exerted on it. This behaviour, which was also noted by Jeffrey & Onishi (1981), is different from that for the creeping motion of a sphere in the vicinity of a plane (O'Neill 1964; O'Neill & Stewartson 1967; Goldman, Cox & Brenner 1967).

For the two-dimensional streaming motion of an infinite circular cylinder in an unbounded fluid, namely, the case of $\lambda = 0$ or $\psi_0 \to \infty$, all of the coefficients given by (2.11) vanish and there exists no solution of the creeping motion equations (known as Stokes' paradox). Treating a variety of problems in slender-body Stokes flow, Cox (1970) obtained the following asymptotic formula for the drag force per unit length acting on a relatively long circular cylinder of finite length in an unbounded fluid:

$$\boldsymbol{F} = 4\pi\eta\{[\ln(2l/a) - \tfrac{1}{2}]^{-1} + O[\ln(l/a)]^{-3}\}\, \boldsymbol{U}, \tag{2.16}$$

where $\boldsymbol{U}$ is the translational velocity of the cylinder (perpendicular to its axis) and l is the length of the cylinder.

3. Electrophoresis of a circular cylinder parallel to a dielectric plane

We now consider the two-dimensional electrophoretic motion of an infinite non-conducting cylinder of radius a (represented by $\psi = \psi_0$) in the direction normal to its axis and parallel to an infinite dielectric plane (located at $x = 0$). The applied electric field is constant and equals $E_\infty \boldsymbol{e}_y$. The Debye length is assumed to be much smaller than the cylinder radius and the spacing between solid surfaces. Our objective is to determine the correction to the Smoluchowski equation (1.1) for the cylindrical particle due to the presence of the planar wall.

3.1. *Electrical potential distribution*

The fluid outside the thin double layer is neutral and of constant conductivity; hence, the electrical potential distribution $\Phi(\boldsymbol{x})$ is governed by the Laplace equation:

$$\nabla^2\Phi = 0, \tag{3.1}$$

where ∇^2 is given by (2.6*b*). The local electric field $\boldsymbol{E}(\boldsymbol{x})$ equals $-\nabla\Phi$. Since the potential gradient far away from the cylinder approaches the applied electric field and both the cylinder and the wall are assumed to be perfectly insulating, the electrical potential is subject to the boundary conditions

$$\boldsymbol{e}_\psi \cdot \nabla\Phi = 0 \qquad \text{at} \quad \psi = \psi_0, \tag{3.2a}$$

$$\boldsymbol{e}_\psi \cdot \nabla\Phi = 0 \qquad \text{at} \quad \psi = 0, \tag{3.2b}$$

$$\Phi \to -E_\infty y \quad \text{as} \quad (x^2+y^2)^{\frac{1}{2}} \to \infty \text{ and } x \geqslant 0. \tag{3.2c}$$

A general solution to (3.1) suitable for satisfying (3.2) is (Umemura 1982)

$$\Phi = G_0 + G_1\psi + \sum_{n=1}^{\infty} [(R_n \cosh n\psi + S_n \sinh n\psi)\cos n\xi + (R'_n \cosh n\psi + S'_n \sinh n\psi)\sin n\xi] - cE_\infty(\cosh\psi - \cos\xi)^{-1}\sin\xi, \tag{3.3}$$

in which the last term is the electrical potential distribution that would exit in the absence of the cylinder. Applying boundary conditions (3.2), one can easily obtain the coefficients in (3.3) as

$$G_0 = G_1 = R_n = S_n = S'_n = 0 \tag{3.4a}$$

and

$$R'_n = -4cE_\infty(\mathrm{e}^{2n\psi_0} - 1)^{-1}, \tag{3.4b}$$

for $n \geqslant 1$. Substituting (3.4) into (3.3), we have the solution for the electrical potential in the fluid phase

$$\Phi = -2cE_\infty \sum_{n=1}^{\infty} \frac{\mathrm{e}^{-n\psi_0}}{\sinh n\psi_0} \cosh n\psi \sin n\xi - cE_\infty \frac{\sin\xi}{\cosh\psi - \cos\xi}. \tag{3.5}$$

The electric field function V is related to the electrical potential by the formulae

$$\frac{\partial\Phi}{\partial x} = \frac{\partial V}{\partial y}, \quad \frac{\partial\Phi}{\partial y} = -\frac{\partial V}{\partial x}. \tag{3.6a, b}$$

Using (2.1) and the chain rule, one can easily find that the above relationships are equivalent to

$$\frac{\partial\Phi}{\partial\xi} = \frac{\partial V}{\partial\psi}, \quad \frac{\partial\Phi}{\partial\psi} = -\frac{\partial V}{\partial\xi}. \tag{3.7a, b}$$

The imaginary part of the complex potential satisfying the above Cauchy–Riemann equations and with its real part given by (3.5) is the electric field function:

$$V = -2cE_\infty \sum_{n=1}^{\infty} \frac{\mathrm{e}^{-n\psi_0}}{\sinh n\psi_0} \sinh n\psi \cos n\xi + cE_\infty \frac{\sinh\psi}{\cosh\psi - \cos\xi}. \tag{3.8}$$

3.2. *Fluid velocity distribution*

Having obtained the solution for the electric field, we can now proceed to find the fluid velocity field. Because the Reynolds number associated with electrophoretic motions is small, equations (2.3)–(2.5) apply for the fluid motion outside the thin

double layers. At the surfaces of the cylinder and the planar wall, the electric field acting on the diffuse ions within the double layer produces a relative tangential fluid velocity at the outer boundary of the double layer. This velocity is described by the Helmholtz equation (1.2). Also, a uniform electro-osmotic flow far away from the cylinder is generated by the tangential fluid velocity at the planar surface. Therefore, the boundary conditions for the flow field are

$$\boldsymbol{v} = U_y \boldsymbol{e}_y + a\Omega \boldsymbol{e}_\xi + \frac{\epsilon\zeta_p}{4\pi\eta}\nabla\Phi \quad \text{at} \quad \psi = \psi_0, \tag{3.9a}$$

$$\boldsymbol{v} = \frac{\epsilon\zeta_w}{4\pi\eta}\nabla\Phi \qquad \text{at} \quad \psi = 0, \tag{3.9b}$$

$$\boldsymbol{v} \to \boldsymbol{v}_\infty = -\frac{\epsilon\zeta_w}{4\pi\eta}E_\infty \boldsymbol{e}_y \qquad \text{as} \quad (x^2+y^2)^{\frac{1}{2}} \to \infty \text{ and } x \geqslant 0, \tag{3.9c}$$

where ζ_p and ζ_w are the zeta potentials associated with the cylinder and the planar wall respectively; U_y and Ω are respectively the translational and angular velocities of the electrophoretic cylinder to be determined. Note that the normal component of $\nabla\Phi$ vanishes at the solid surfaces as required by (3.2*a*) and (3.2*b*), and the tangential component of the electric field is obtained from the potential distribution given by (3.5). Because the cylinder is freely suspended in the fluid and the particle 'surface' encloses a neutral body (charged interface plus diffuse ions), the net force and net torque per unit length exerted by the fluid on the cylinder must vanish.

Since the governing equation and the boundary conditions are linear, the total flow can be decomposed into two parts. First, we consider the fluid motion about an infinite cylinder (at $\psi = \psi_0$) moving parallel to the planar wall (at $\psi = 0$) with translational velocity $U_y \boldsymbol{e}_y$ and angular velocity $\Omega \boldsymbol{e}_z$ but with no tangential electrokinetic velocity at the solid surfaces. The stream function for this flow can be obtained by substituting (2.11) into (2.10) and taking $U_x = 0$, with the result

$$\Psi_1 = \frac{a\sinh\psi_0}{\cosh\psi-\cos\xi}\left\{\left(\frac{U_y}{\psi_0}+\frac{a\Omega}{\sinh\psi_0}\right)[\psi(\cosh\psi-\cos\xi)\coth\psi_0-\sinh\psi\coth\psi_0 + \sinh\psi\cos\xi(\cosh\psi\coth\psi_0-\sinh\psi)]-\frac{U_y}{\psi_0}\psi\sinh\psi\right\}. \tag{3.10}$$

The force and torque per unit length on the cylinder are obtained from (2.15) with $U_x = 0$ as

$$\boldsymbol{F}_1 = -\frac{4\pi\eta U_y}{\psi_0}\boldsymbol{e}_y, \tag{3.11a}$$

$$\boldsymbol{T}_1 = -4\pi\eta a^2\Omega\coth\psi_0\,\boldsymbol{e}_z. \tag{3.11b}$$

Next, we consider the flow caused by the electrokinetic tangential velocity at the surface (i.e. outer edge of the double layer) of a stationary cylinder near a planar wall with $\zeta_w = 0$:

$$\boldsymbol{v}_2 = \frac{\epsilon\zeta_p}{4\pi\eta}\nabla\Phi \quad \text{at} \quad \psi = \psi_0, \tag{3.12a}$$

$$\boldsymbol{v}_2 = \boldsymbol{0} \qquad \text{at} \quad \psi = 0, \tag{3.12b}$$

$$\boldsymbol{v}_2 \to \boldsymbol{0} \qquad \text{as} \quad (x^2+y^2)^{\frac{1}{2}} \to \infty \text{ and } x \geqslant 0. \tag{3.12c}$$

Superimposing the velocity field $\boldsymbol{v}_2$ with that derived from (3.10) yields the total velocity field produced by the transverse electrophoretic motion of a non-conducting cylinder parallel to a neutral dielectric plane. By obtaining the force and torque exerted on the stationary cylinder, individually adding these to the force and torque given by (3.11) and equating the results to zero, the translational and rotational velocities of the cylinder will result. For the more general case that $\zeta_w \neq 0$, the wall correction for the particle velocities can be obtained by replacing the variable ζ_p in the results for the neutral plane with the difference in zeta potential between the cylinder and the planar wall, $\zeta_p - \zeta_w$ (Keh & Anderson 1985; Keh & Chen 1988).

The stream function Ψ_2 for the flow caused by the electrokinetic velocity at the surface of the stationary cylinder can also be expressed by (2.10), and the coefficients A, B, C, D, a_n, b_n, c_n, d_n, a'_n, b'_n, c'_n and d'_n should be determined by the boundary conditions (3.12). The procedure to obtain these coefficients by applying (3.12) to (2.10) and using (3.5), (2.6a) and (2.8) is straightforward but tedious, with the results

$$A = U_0 \frac{4\psi_0 - \sinh 4\psi_0}{4\psi_0 \sinh^2 \psi_0 \sinh 2\psi_0}, \quad B = -A, \tag{3.13a, b}$$

$$C = U_0 \frac{\coth 2\psi_0}{\psi_0}, \quad D = 0, \tag{3.13c, d}$$

$$a_1 = U_0 \frac{\sinh \psi_0 \cosh 2\psi_0 - 2\psi_0 \cosh \psi_0}{2\psi_0 \sinh \psi_0 \sinh 2\psi_0}, \tag{3.13e}$$

$$b_1 = \tfrac{1}{2}A, \quad c_1 = -a_1, \tag{3.13f, g}$$

$$a_n = U_0 \frac{e^{-n\psi_0}[(n-1)\sinh(n+1)\psi_0 - (n+1)\sinh(n-1)\psi_0]}{4(\sinh^2 n\psi_0 - n^2 \sinh^2 \psi_0)} [2\sinh \psi_0 + 2n \cosh \psi_0 \coth n\psi_0 - (n+1)\, e^{-\psi_0} \coth(n+1)\psi_0 - (n-1)\, e^{\psi_0} \coth(n-1)\psi_0] \quad (n \geqslant 2), \tag{3.13h}$$

$$b_n = \frac{(n-1)[\cosh(n+1)\psi_0 - \cosh(n-1)\psi_0]}{(n+1)\sinh(n-1)\psi_0 - (n-1)\sinh(n+1)\psi_0} a_n \quad (n \geqslant 2), \tag{3.13i}$$

$$c_n = -a_n, \quad d_n = -\frac{n+1}{n-1} b_n \quad (n \geqslant 2), \tag{3.13j, k}$$

$$a'_n = b'_n = c'_n = d'_n = 0 \quad (n \geqslant 1), \tag{3.13l}$$

where $U_0 = \epsilon \zeta_p E_\infty / 4\pi\eta$.

The force and torque per unit length exerted on the stationary cylinder by the fluid due to the electrokinetic motion can be obtained by the substitution of (3.13a, c, d) into (2.14). The results are

$$\boldsymbol{F}_2 = 4\pi\eta U_0 \frac{\coth 2\psi_0}{\psi_0} \boldsymbol{e}_y, \tag{3.14a}$$

$$\boldsymbol{T}_2 = -\frac{4\pi\eta a U_0}{\sinh \psi_0 \sinh 2\psi_0} \boldsymbol{e}_z. \tag{3.14b}$$

3.3. *Derivation of the particle velocities*

Since the net force and net torque acting on the electrophoretic cylinder must vanish, we have

$$\boldsymbol{F}_1 + \boldsymbol{F}_2 = \boldsymbol{0}, \quad \boldsymbol{T}_1 + \boldsymbol{T}_2 = \boldsymbol{0}. \tag{3.15a, b}$$

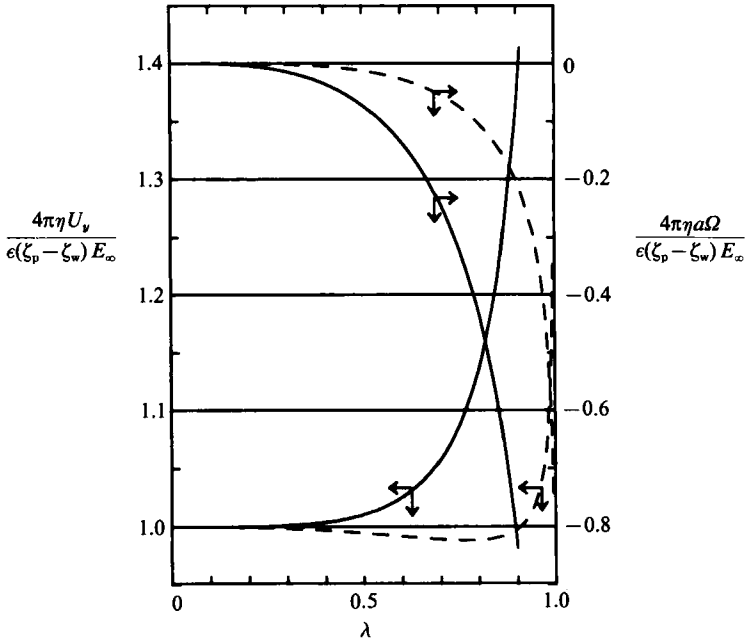

FIGURE 2. Plots of the translational and rotational velocities of a cylinder (solid curves, as computed from (3.17)) and of a sphere (dashed curves, obtained from Keh & Chen 1988) undergoing electrophoresis parallel to a dielectric plane, versus the separation parameter λ.

To determine the translational velocity U_y and rotational velocity Ω of the cylinder near a neutral planar wall, the above equations must be solved after substituting (3.11) and (3.14) into them. The results are

$$U_y = \frac{\epsilon\zeta_p}{4\pi\eta}E_\infty \coth 2\psi_0, \quad \Omega = -\frac{\epsilon\zeta_p}{4\pi\eta a}E_\infty \frac{\operatorname{sech}\psi_0}{\sinh 2\psi_0}. \tag{3.16a, b}$$

When the planar surface has a finite zeta potential ζ_w, the translational and angular velocities of the cylinder become

$$U_y = \frac{\epsilon(\zeta_p-\zeta_w)}{4\pi\eta}E_\infty \coth 2\psi_0, \quad \Omega = -\frac{\epsilon(\zeta_p-\zeta_w)}{4\pi\eta a}E_\infty \frac{\operatorname{sech}\psi_0}{\sinh 2\psi_0}. \tag{3.17a, b}$$

The connection between ψ_0 and the separation parameter λ is given by (2.2).

3.4. *Results and discussion*

Values of the normalized translational and rotational velocities of the electrophoretic cylinder evaluated from (3.17) with various values of separation parameter λ are plotted by the solid curves in figure 2. For the corresponding electrophoretic motion of a sphere parallel to a dielectric plane, a combined analytical–numerical solution was developed by using spherical bipolar coordinates (Keh & Chen 1988). The wall-corrected reduced translational and angular velocities of the electrophoretic sphere as a function of λ (in this case λ is the ratio of the sphere radius to the distance of the sphere centre from the plane wall) are drawn by the dashed curves in figure 2 for comparison. As expected, both the cylindrical and spherical particles will move (without rotation) with the velocity that would exist in the absence of the wall, given

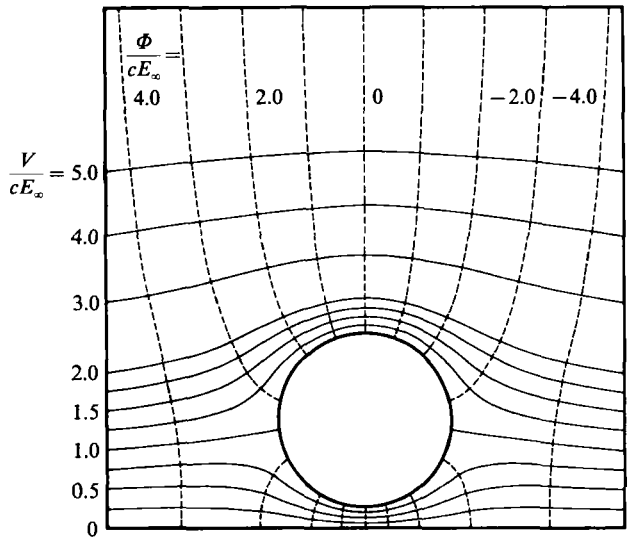

FIGURE 3. Electric field lines (solid curves) and equipotential lines (dashed curves) for the electrophoretic motion of a cylinder parallel to a dielectric plane with $\lambda = 0.8$.

by the Smoluchowski equation (1.1), as $\lambda \to 0$. Note that an important difference between electrophoresis and sedimentation in the unbounded case is that a solution to Stokes flow for an infinite cylinder exists for the former but not for the latter.

Examination of the results shown in figure 2 reveals an interesting feature. The electrophoretic mobility of the cylinder is a monotonic *increasing* function of λ and becomes infinity in the limit of $\lambda \to 1$. The behaviour is understandable because the crowding of the electric field lines when they squeeze between the particle and the wall increases the local electrical force driving the particles' motion (Keh & Chen 1988). In figure 3, the electric field lines and equipotential curves for the case of a cylinder with $\lambda = 0.8$ are presented using (3.5) and (3.8). The local electric field at the particle 'surface' on the near side to the planar wall is enhanced in comparison with that on the far side. Obviously, the influence of this enhancement on the particle velocity is very important and much stronger than the effect of viscous retardation caused by the wall.

On the other hand, the electrophoretic mobility of the sphere is a monotonic decreasing function of λ for all $\lambda \leqslant 0.77$. In this region, the effect of the viscous drag of the wall is stronger than the wall effect on the interaction between the sphere and the electric field. When the gap width between solid surfaces is small, the effect of the enhancement of the local electric field at the particle surface becomes dominant and the electrophoretic mobility of the sphere increases with increasing λ. Note that the wall effect on the electrophoretic mobility of a cylinder (76% increase for $\lambda = 0.95$) is much more significant than that on a sphere (2.2% increase for $\lambda = 0.95$). This is because the effective wall-interaction area that offers electrostatic enhancement and hydrodynamic resistance to the motion of a cylinder is much larger than that to the movement of a sphere.

Although an infinite cylinder migrating parallel to a planar wall under a body-force field does not rotate (as we have seen in §2), an electrophoretic cylinder or sphere will rotate about an axis which is perpendicular to the direction of the applied electric field and parallel to the planar wall. The direction of rotation is opposite to that for a sphere sedimenting in the same direction parallel to a plane. A discussion

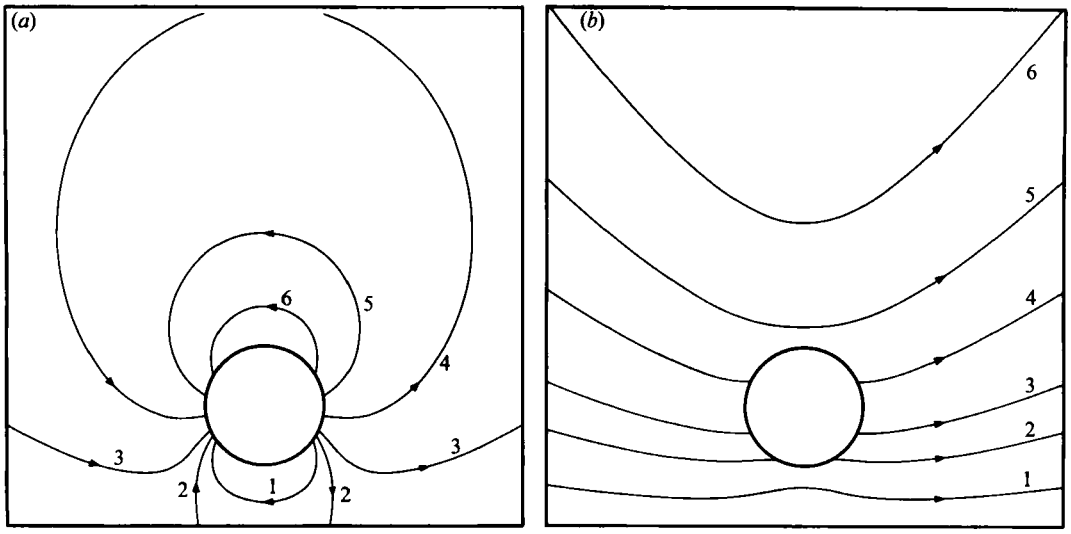

FIGURE 4. Streamlines around a cylinder moving parallel to a plane wall with $\lambda = 0.5$. (*a*) Electrophoresis. Curve 1, $4\pi\eta\Psi/c\epsilon\zeta_p E_\infty = 0.05$; 2, 0; 3, -0.05; 4, -0.2; 5, -0.4; 6, -0.6. (*b*) Sedimentation. Curve 1, $\Psi/cU_y = -0.05$; 2, -0.25; 3, -0.5; 4, -1.0; 5, -1.5; 6, -2.0.

of this counter-intuitive result for electrophoretic particles was provided by Keh & Chen (1988). In spite of that a torque-free sphere has a lower electrophoretic mobility near the planar wall than that for a non-rotating sphere (Keh & Chen 1988), which is also opposite to the behaviour for a sphere moving under gravity near boundaries, the electrophoretic mobility of an infinite cylinder near the wall is independent of the external torque exerted on the cylinder. This phenomenon is understandable knowing the fact that there is no coupling between translation and rotation for the creeping motion of a cylinder near a planar wall considered in §2.

For the electrophoretic motion of a cylinder in a transverse electric field parallel to a neutral planar wall, the stream function for the flowing fluid can be evaluated from the combination of Ψ_1 given by (3.10) and Ψ_2 in the form of (2.10) with coefficients given by (3.13). The streamlines for the situation when the radius of the cylinder is equal to the surface-to-surface distance between the cylinder and the wall are depicted in figure 4(*a*). The contour pattern shows the distortion of fluid recirculation around the cylinder (which corresponds to a potential doublet) due to the planar wall in the proximity. Note that the fluid flow in figure 4(*a*) contains two stagnation points on the wall where the two recirculation regions meet each other. If s denotes the distance between either of the stagnation points and the origin of the coordinate system, then the value of s/d depends on the separation parameter λ, but is independent of the electrophoretic velocity of the particle. Here we present the results of s/d versus λ in the first two columns of table 1, from which a monotonic decreasing function is observed.

Figure 4(*b*) corresponds to the streamline pattern for the movement of a cylinder driven by a body force parallel to a planar wall, which can be made using the formula given by (3.10). In comparison with the situation of electrophoresis, the fluid motion in figure 4(*b*) contains only a global flow and no stagnation point appears on the wall. This difference is because the disturbance to the fluid velocity field caused by an electrophoretic particle, which is that of a potential dipole, decays much faster than that caused by a stokeslet.

λ	$\frac{s}{d}$	$\frac{b}{d}$	$\frac{h}{d}$
0.1	0.5770	1.4214	2.0114
0.2	0.5745	1.4134	1.9985
0.3	0.5703	1.3916	1.9690
0.4	0.5629	1.3564	1.9289
0.5	0.5508	1.3004	1.8739
0.6	0.5318	1.2224	1.7887
0.7	0.5019	1.1084	1.7001
0.8	0.4535	0.9337	1.8001
0.9	0.3649	0.6720	1.9000
0.95	0.2811	0.5124	1.9500

TABLE 1. The variations of s/d, b/d and h/d with respect to the separation parameter λ. s is the distance of either stagnation point on the dielectric plane (in figure 4a) from the origin of the coordinate system. b and h are the distances of stagnation points on the conducting plane and on the axis, respectively (in figure 7a), from the origin of the coordinate system.

4. Electrophoresis of a circular cylinder normal to a conducting plane

In this section we consider the two-dimensional electrophoretic motion of an infinite non-conducting cylinder of radius a in the direction perpendicular to its axis and to an infinite conducting plane. A constant electric field $E_\infty \boldsymbol{e}_x$ is imposed normal to the plane at $x = 0$. As in the previous section, the assumption of a thin electrical double layer is employed. Our purpose is to find the wall-corrected electrophoretic velocity of the cylindrical particle.

4.1. *Electrical potential distribution*

The electrostatic equation governing the potential distribution $\Phi(\boldsymbol{x})$ is the Laplace equation (3.1). The planar wall is assumed to be perfectly conducting and its potential is taken as zero for convenience. Thus, the boundary conditions for $\Phi(\boldsymbol{x})$ are

$$\boldsymbol{e}_\psi \cdot \nabla\Phi = 0 \quad \text{at} \quad \psi = \psi_0, \tag{4.1a}$$

$$\Phi = 0 \quad \text{at} \quad \psi = 0, \tag{4.1b}$$

$$\Phi \to -E_\infty x \quad \text{as} \quad (x^2+y^2)^{\frac{1}{2}} \to \infty \text{ and } x \geqslant 0. \tag{4.1c}$$

The solution form for the electrical potential is still given by (3.3). Applying (4.1) to (3.3) and utilizing the requirement that the potential field is symmetric about the x-axis, one obtains the unknown coefficients in (3.3) as

$$G_0 = G_1 = R_n = R'_n = S'_n = 0 \tag{4.2a}$$

and

$$S_n = -4cE_\infty(\mathrm{e}^{2n\psi_0}+1)^{-1}, \tag{4.2b}$$

for $n \geqslant 1$.

Substitution of (4.2) into (3.3) leads to the solution for the electrical potential in the fluid phase:

$$\Phi = -2cE_\infty \sum_{n=1}^{\infty} \frac{\mathrm{e}^{-n\psi_0}}{\cosh n\psi_0} \sinh n\psi \cos n\xi - cE_\infty \frac{\sinh\psi}{\cosh\psi - \cos\xi}. \tag{4.3}$$

The corresponding electric field function, which satisfies (3.7), is

$$V = 2cE_\infty \sum_{n=1}^{\infty} \frac{\mathrm{e}^{-n\psi_0}}{\cosh n\psi_0} \cosh n\psi \sin n\xi - cE_\infty \frac{\sin\xi}{\cosh\psi - \cos\xi}. \tag{4.4}$$

4.2. *Fluid velocity distribution*

The fluid motion outside the thin double layer is governed by (2.5) and subject to the following boundary conditions:

$$\boldsymbol{v} = U_x \boldsymbol{e}_x + \frac{\epsilon\zeta_p}{4\pi\eta}\nabla\Phi \quad \text{at} \quad \psi = \psi_0, \tag{4.5a}$$

$$\boldsymbol{v} = \boldsymbol{0} \quad \text{at} \quad \psi = 0, \tag{4.5b}$$

$$\boldsymbol{v} \to \boldsymbol{0} \quad \text{as} \quad (x^2+y^2)^{\frac{1}{2}} \to \infty \text{ and } x \geqslant 0, \tag{4.5c}$$

where U_x is the electrophoretic velocity of the cylindrical particle to be determined. The cylinder does not rotate owing to the symmetry of the flow field about the x-axis. The potential distribution in (4.5a) is given by (4.3).

Similarly to the case considered in the previous section, the total flow can be decomposed into two parts: the creeping flow about an infinite cylinder translating perpendicular to its axis and a planar wall with a velocity $U_x \mathrm{e}_x$ and the fluid motion produced by the tangential electrokinetic velocity at the surface of a stationary cylinder near a planar wall. The stream function for the first part can be obtained by substituting (2.11) into (2.10) and taking $U_y = \Omega = 0$, with the result

$$\Psi_1 = \frac{aU_x \sinh\psi_0 \sin\xi}{(\cosh\psi - \cos\xi)(\psi_0 - \tanh\psi_0)}(\psi - \tfrac{1}{2}\sinh 2\psi + \tanh\psi_0 \sinh^2\psi). \tag{4.6}$$

Equation (2.15a) with $U_y = 0$ gives the drag force per unit length exerted by the fluid on the cylinder:

$$\boldsymbol{F}_1 = -\frac{4\pi\eta U_x}{\psi_0 - \tanh\psi_0}\boldsymbol{e}_x. \tag{4.7}$$

There is no torque acting on the translating cylinder.

The velocity field $\boldsymbol{v}_2$ for the second part of the total flow is subject to the boundary conditions given by (3.12) with Φ provided by (4.3). The stream function Ψ_2 associated with $\boldsymbol{v}_2$ can also be expressed by (2.10), and the coefficients $A, B, C, \ldots$, *etc.* should be determined by applying (3.12) to (2.10) and using (4.3), (2.6a) and (2.8). After considerable algebraic manipulation, one obtains

$$A = B = C = 0, \tag{4.8a}$$

$$D = U_0 \frac{4\mathrm{e}^{-\psi_0}(1-\mathrm{e}^{-\psi_0})\sinh^3\psi_0}{1+\psi_0\sinh 2\psi_0 - \cosh 2\psi_0}, \tag{4.8b}$$

$$a_n = b_n = c_n = d_n = 0 \quad (n \geqslant 1), \tag{4.8c}$$

$$a_1' = \frac{2\psi_0 - \sinh 2\psi_0}{2(\cosh 2\psi_0 - 1)}D, \tag{4.8d}$$

$$b_1' = \tfrac{1}{2}D, \quad c_1' = -a_1', \tag{4.8e,f}$$

$$a_n' = U_0 \frac{\mathrm{e}^{-n\psi_0}[(n+1)\sinh(n-1)\psi_0 - (n-1)\sinh(n+1)\psi_0]}{4\cosh n\psi_0(\sinh^2 n\psi_0 - n^2\sinh^2\psi_0)}$$
$$\times[(n+1)(1-\mathrm{e}^{-\psi_0})\sinh(n+1)\psi_0 + (n-1)(1-\mathrm{e}^{\psi_0})\sinh(n-1)\psi_0] \quad (n \geqslant 2), \tag{4.8g}$$

$$b_n' = \frac{(n-1)[\cosh(n+1)\psi_0 - \cosh(n-1)\psi_0]}{(n+1)\sinh(n-1)\psi_0 - (n-1)\sinh(n+1)\psi_0}a_n' \quad (n \geqslant 2), \tag{4.8h}$$

$$c_n' = -a_n', \quad d_n' = -\frac{n+1}{n-1}b_n' \quad (n \geqslant 2), \tag{4.8i,j}$$

where $U_0 = \epsilon\zeta_p E_\infty / 4\pi\eta$.

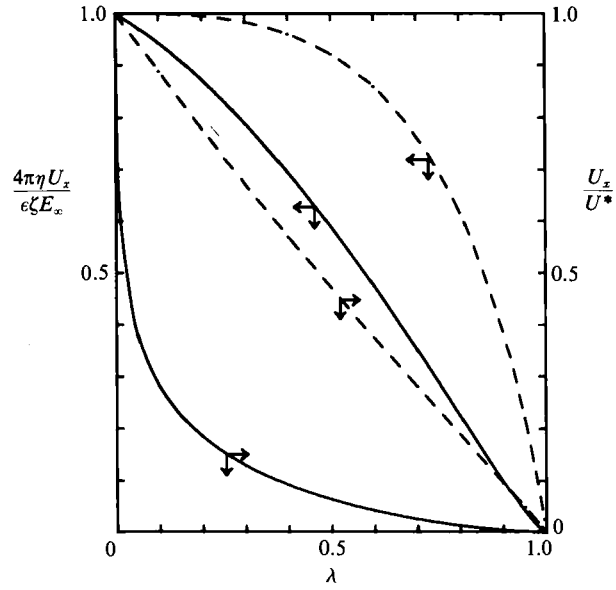

FIGURE 5. Plots of the normalized electrophoretic and hydrodynamic mobilities of a cylinder (solid curves, as computed from (4.10) and (4.7)) and of a sphere (dashed curves, obtained from Keh & Lien 1991 and Brenner 1961) in the direction normal to a plane wall, versus the separation parameter λ.

The force per unit length acting on the stationary cylinder due to the flow caused by the electrokinetic velocity at the surface of the cylinder, which can be obtained by the substitution of (4.8a, b) into (2.14a), is

$$\boldsymbol{F}_2 = 4\pi\eta U_0 \frac{4\mathrm{e}^{-\psi_0}(1-\mathrm{e}^{-\psi_0})\sinh^3\psi_0}{1+\psi_0\sinh 2\psi_0-\cosh 2\psi_0}\boldsymbol{e}_x. \tag{4.9}$$

4.3. *Derivation of the particle velocity*

Because the electrophoretic cylinder is freely suspended in the fluid, the net force exerted on the cylinder (plus the thin diffuse layer) vanishes. Substitution of (4.7) and (4.9) into (3.15a) yields the electrophoretic velocity U_x of the cylinder near a conducting plane:

$$U_x = \frac{\epsilon\zeta_{\mathrm{p}}}{4\pi\eta}E_\infty \frac{4\mathrm{e}^{-\psi_0}(1-\mathrm{e}^{-\psi_0})(\psi_0-\tanh\psi_0)\sinh^3\psi_0}{1+\psi_0\sinh 2\psi_0-\cosh 2\psi_0}. \tag{4.10}$$

By the linearity of the problem, the same magnitude of the particle velocity is predicted for a given separation parameter λ, which is related to ψ_0 by (2.2), whether the particle is approaching the planar wall or receding from it.

4.4. *Results and discussion*

Numerical values for the wall-corrected reduced electrophoretic mobility of a cylinder, calculated from (4.10) for various values of λ, are plotted by a solid curve in figure 5. The corresponding results for the electrophoretic motion of a sphere normal to a planar wall obtained by using spherical bipolar coordinates (Keh & Lien

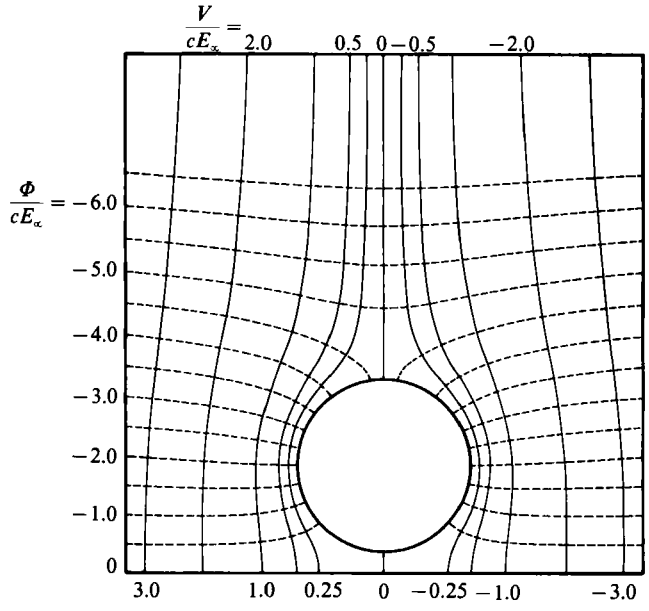

FIGURE 6. Electric field lines (solid curves) and equipotential lines (dashed curves) for the electrophoretic motion of a cylinder normal to a conducting plane with $\lambda = 0.8$.

1989, 1991) are drawn by a dashed curve in the same figure for comparison. When $\lambda \to 0$, the particle moves with the velocity given by Smoluchowski's equation. The electrophoretic mobility then decreases steadily as the particle approaches the wall (with increasing λ) going to zero in the limit. As a comparison to figure 3, the electric field lines and equipotential curves for the case of a cylinder (upon which the electric field is imposed perpendicular to a conducting plane) with $\lambda = 0.8$ are drawn in figure 6 using (4.3) and (4.4). The local electric field at the particle surface on the side next to the wall is depressed compared with that on the far side. This demonstrates that the effect of the conducting plane on the interaction between particle and electric field will reduce the electrophoretic velocity of the particle. Similarly to the electrophoretic motion of particles parallel to a planar wall considered in §3, the wall effect on the mobility reduction for a cylinder (41% for $\lambda = 0.5$) is much more significant than that for a sphere (7.9% for $\lambda = 0.5$).

For the motion of an infinite cylinder on which a constant transverse body force per unit length $F\boldsymbol{e}_x$ (e.g. a gravitational field) is imposed normal to a planar wall, the particle velocity can be determined by (4.7) with $\boldsymbol{F}_1$ replaced by $-F\boldsymbol{e}_x$. The creeping-motion velocity of a sphere migrating normal to a planar wall driven by a body force was obtained by Maude (1961) and Brenner (1961). The numerical results for the wall-corrected normalized hydrodynamic mobilities of the cylindrical and spherical particles for various values of λ are also presented in figure 5 for comparison. Since there exists no solution of the Stokes equations for the two-dimensional streaming motion perpendicular to the axis of an infinite cylinder in an unbounded fluid, the asymptotic formula given by (2.16) is used to determine the mobility of an isolated cylindrical particle. A length-to-radius ratio (l/a) of the finite cylinder equal to 1000 is chosen in (2.16) to calculate the characteristic velocity U^*:

$$U^* \approx 7.1009 \frac{F}{4\pi\eta}. \tag{4.11}$$

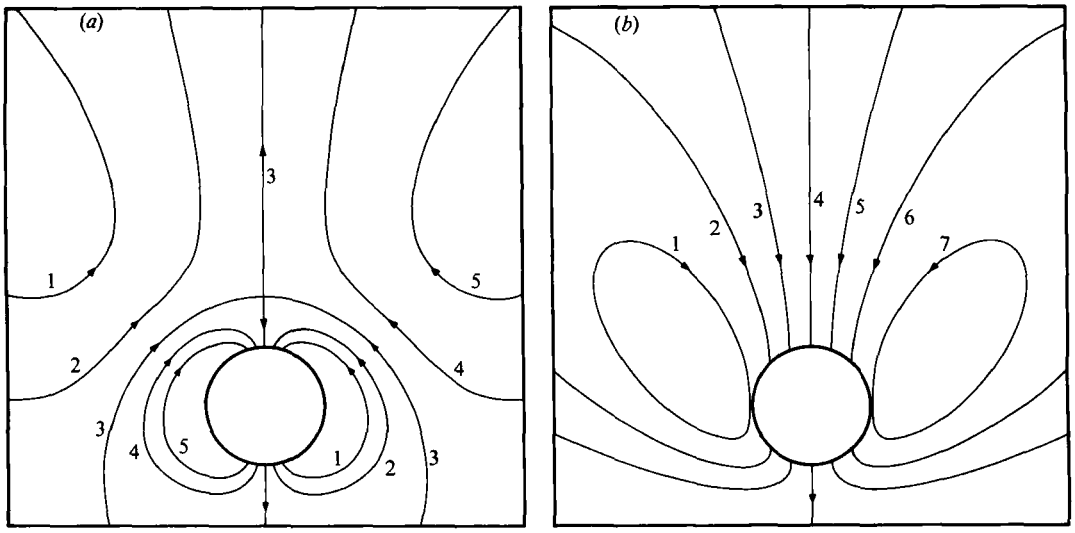

FIGURE 7. Streamlines around a cylinder migrating normal to a plane wall with $\lambda = 0.5$. (*a*) Electrophoresis. Curve 1, $4\pi\eta\Psi/c\epsilon\zeta E_\infty = -0.10$; 2, -0.05; 3, 0; 4, 0.05; 5, 0.10. (*b*) Sedimentation. Curve 1, $\Psi/cU_x = 0.6$; 2, 0.4; 3, 0.2; 4, 0; 5, -0.2; 6, -0.4; 7, -0.6.

In figure 5, we restrict the comparison to $\lambda \gg a/l$ so that end effects of the cylinder are unimportant. For the creeping motion of a sphere, the characteristic velocity U^* is related to the applied force by the Stokes law. Obviously, the wall effect on electrophoresis is much weaker than on a sedimenting particle. Also, the reduction in hydrodynamic mobility caused by a nearby planar wall is much more significant for a cylinder than for a sphere.

The stream function for the flow field generated by the electrophoretic motion of a cylinder in a transverse electric field normal to a planar wall can be evaluated from the combination of Ψ_1 given by (4.6) and Ψ_2 given by (2.10) and (4.8). In figure 7(*a*), the streamline pattern for the case of $\lambda = 0.5$ is drawn. In addition to the local 'inner' fluid recirculation in the vicinity of the cylinder, there are two symmetric 'outer' recirculation regions extending to the whole remaining fluid phase. The direction of this outer recirculation near the axis of symmetry (x-axis) is opposite to that of the particle's movement. Note that, in figure 7(*a*), three stagnation points appear on the planar wall: one is at the origin of the coordinate system, the other two are on each side of it at a distance b from the origin. Also, there is one more stagnation point on the axis of symmetry at a distance h from the plane. The circulating streamline $\Psi = 0$ intersects the axis at this point orthogonally. The values of b/d and h/d depend on λ, but are independent of the particle velocity. In table 1 we also list the results for b/d and h/d for various values of λ. For b/d versus λ, a monotonic decreasing function is obtained. When $\lambda \geqslant 0.7$, $h/d \approx 1+\lambda$ and the stagnation point on the axis is very close to the far-side pole of the particle.

In figure 7(*b*), the situation for a cylinder sedimenting perpendicular to its axis and to a planar wall is considered. The stream function for this case can be evaluated from (4.6). Contrary to the streamline pattern for electrophoresis, there is no inner-and-outer recirculation or stagnation point on the plane other than the origin of the coordinate system.

5. Summary

In this paper, the exact solutions for the problem of two-dimensional electrophoretic motion of a cylindrical particle in the presence of a plane wall have been obtained using bipolar coordinates in two fundamental cases: migration occurring parallel to a dielectric plane and movement normal to a conducting wall. Throughout the analysis, the assumption of thin double layers adjacent to solid surfaces is employed. Some interesting results which differ significantly from those of the corresponding sedimentation problem have emerged. When the electric field is applied parallel to a plane wall, the magnitudes of both the electrophoretic mobility and the angular velocity of the cylinder increase monotonically as the particle approaches the wall and become infinity as $\lambda \to 1$. This behaviour is due to the feature of squeezed electric field lines in the gap between the particle and the wall. On the other hand, the mobility of a cylinder undergoing electrophoresis normal to a plane wall is a monotonic decreasing function of the separation parameter λ and vanishes in the limit of $\lambda = 1$, because the wall effect on the interaction between particle and electric field in this situation is to decrease the particle velocity. The stream function for the fluid flow in two representative cases of electrophoresis has been depicted in figures 4(*a*) and 7(*a*), while the streamline pattern for the corresponding cases of sedimentation is shown in figures 4(*b*) and 7(*b*) for comparison.

We have seen in figures 2 and 5 that the boundary effects on the electrophoretic motion of a cylinder are much more significant than those of a sphere. It would be of interest to know how a plane wall affects the electrophoresis of other non-spherical particles, say, ellipsoids of revolution. This problem, which requires a combined analytical–numerical solution procedure, is now under investigation.

This research was supported by the National Science Council of the Republic of China.

REFERENCES

Brenner, H. 1961 The slow motion of a sphere through a viscous fluid towards a plane surface. *Chem. Engng Sci.* **16**, 242.

Chen, S. B. & Keh, H. J. 1988 Electrophoresis in a dilute dispersion of colloidal spheres. *AIChE J.* **34**, 1075.

Cox, R. G. 1970 The motion of long slender bodies in a viscous fluid. Part 1. General theory. *J. Fluid Mech.* **44**, 791.

Fair, M. C. & Anderson, J. L. 1989 Electrophoresis of nonuniformly charged ellipsoidal particles. *J. Colloid Interface Sci.* **127**, 388.

Goldman, A. J., Cox, R. G. & Brenner, H. 1967 Slow viscous motion of a sphere parallel to a plane wall. I. Motion through a quiescent fluid. *Chem. Engng Sci.* **22**, 637.

Happel, J. & Brenner, H. 1983 *Low Reynolds Number Hydrodynamics.* Martinus Nijhoff.

Henry, D. C. 1931 The cataphoresis of suspended particles. Part I. The equation of cataphoresis. *Proc. R. Soc. Lond.* A **133**, 106.

Jeffery, G. B. 1922 The rotation of two circular cylinders in a viscous fluid. *Proc. R. Soc. Lond.* A **101**, 169.

Jeffrey, D. J. & Onishi, Y. 1981 The slow motion of a cylinder next to a plane wall. *Q. J. Mech. Appl. Maths* **34**, 129.

Keh, H. J. & Anderson, J. L. 1985 Boundary effects on the electrophoretic motion of colloidal spheres. *J. Fluid Mech.* **153**, 417.

Keh, H. J. & Chen, S. B. 1988 Electrophoresis of a colloidal sphere parallel to a dielectric plane. *J. Fluid Mech.* **194**, 377.

KEH, H. J. & LIEN, L. C. 1989 Electrophoresis of a dielectric sphere normal to a conducting plane. *J. Chinese Inst. Chem. Engrs* **20**, 283.

KEH, H. J. & LIEN, L. C. 1991 Electrophoresis of a colloidal sphere along the axis of a circular orifice or a circular disk. *J. Fluid Mech.* **224**, 305.

KEH, H. J. & YANG, F. R. 1990 Particle interactions in electrophoresis. III. Axisymmetric motion of multiple spheres. *J. Colloid Interface Sci.* **139**, 105.

MAUDE, A. D. 1961 End effects in a falling-sphere viscometer. *Br. J. Appl. Phys.* **12**, 293.

MORRISON, F. A. 1970 Electrophoresis of a particle of arbitrary shape. *J. Colloid Interface Sci.* **34**, 210.

MORRISON, F. A. 1971 Transient electrophoresis of an arbitrarily oriented cylinder. *J. Colloid Interface Sci.* **36**, 139.

MORRISON, F. A. & STUKEL, J. J. 1970 Electrophoresis of insulating sphere normal to a conducting plane. *J. Colloid Interface Sci.* **33**, 88.

O'NEILL, M. E. 1964 A slow motion of viscous liquid caused by a slowly moving solid sphere. *Mathematika* **11**, 67.

O'NEILL, M. E. & STEWARTSON, K. 1967 On the slow motion of a sphere parallel to a nearby plane wall. *J. Fluid Mech.* **27**, 705.

REED, L. D. & MORRISON, F. A. 1976 Hydrodynamic interactions in electrophoresis. *J. Colloid Interface Sci.* **54**, 117.

STIGTER, D. 1978 Electrophoresis of highly charged colloidal cylinders in univalent salt solution. 1. Mobility in transverse field. *J. Phys. Chem.* **82**, 1417.

TEUBNER, M. 1982 The motion of charge colloidal particles in electric fields. *J. Chem. Phys.* **76**, 5564.

UMEMURA, A. 1982 Matched-asymptotic analysis of low-Reynolds-number flow past two equal circular cylinders. *J. Fluid Mech.* **121**, 345.

WAKIYA, S. 1975 Application of bipolar coordinates to the two-dimensional creeping motion of a liquid. II. Some problems for two circular cylinders in viscous fluid. *J. Phys. Soc. Japan* **39**, 1603.

YOON, B. J. & KIM, S. 1989 Electrophoresis of spheroidal particles. *J. Colloid Interface Sci.* **128**, 275.